Title: Targeting host deoxycytidine kinase mitigates *Staphylococcus aureus* abscess formation

Authors: Volker Winstel[1,2]*, Evan R. Abt[3], Thuc M. Le[3], Caius G. Radu[3]

Affiliations:

[1] Research Group Pathogenesis of Bacterial Infections; TWINCORE, Centre for Experimental and Clinical Infection Research, a joint venture between the Hannover Medical School and the Helmholtz Centre for Infection Research, Hannover, Germany

[2] Institute of Medical Microbiology and Hospital Epidemiology, Hannover Medical School, Hannover, Germany

[3] Department of Molecular and Medical Pharmacology, David Geffen School of Medicine, UCLA, Los Angeles, United States of America

* Address **correspondence** to Volker Winstel: winstel.volker@mh-hannover.de

Institute of Medical Microbiology and Hospital Epidemiology, Hannover Medical School
Carl-Neuberg-Str. 1, 30625 Hannover, Germany
Phone: +49 511 22002 7220 / Fax: +49 511 22002 7186

Abstract

Host-directed therapy (HDT) is an emerging approach to overcome antimicrobial resistance in pathogenic microorganisms. Specifically, HDT targets host-encoded factors required for pathogen replication and survival without interfering with microbial growth or metabolism, thereby eliminating the risk of resistance development. By applying HDT and a drug repurposing approach, we demonstrate that (*R*)-DI-87, a clinical-stage anti-cancer drug and potent inhibitor of mammalian deoxycytidine kinase (dCK), mitigates *Staphylococcus aureus* abscess formation in organ tissues upon invasive bloodstream infection. Mechanistically, (*R*)-DI-87 shields phagocytes from staphylococcal death-effector deoxyribonucleosides that target dCK and the mammalian purine salvage pathway-apoptosis axis. In this manner, (*R*)-DI-87-mediated protection of immune cells amplifies macrophage infiltration into deep-seated abscesses, a phenomenon coupled with enhanced pathogen control, ameliorated immunopathology, and reduced disease severity. Thus, pharmaceutical blockade of dCK represents an advanced anti-infective intervention strategy against which staphylococci cannot develop resistance and may help to fight fatal infectious diseases in hospitalized patients.

Introduction

Hospital- and community-acquired infections caused by antibiotic-resistant bacterial pathogens represent a global public health threat (Wenzel, 2007; GBD 2019 Antimicrobial Resistance Collaborators, 2022a; b). Specifically, infections caused by multidrug-resistant microbes are often associated with increased morbidity and mortality, as compared to infections caused by antibiotic-sensitive strains (Klevens et al., 2008; Yaw et al., 2014; GBD 2019 Antimicrobial Resistance Collaborators, 2022a; b). In addition, the pathology of various bacterial infections includes multifactorial manipulation of host multicellular assemblies that enable pathogen replication, dissemination of disease, and adaptation to new hosts (Foster, 2005; Finlay and McFadden, 2006; Okumura and Nizet, 2014; Thammavongsa et al., 2015). Thus, prevention and therapy of such infections represent a major challenge in clinical practice and frequently require administering last-resort antibiotics such as vancomycin, linezolid, or colistin (Chambers and Deleo, 2009; McKenna, 2013; Tong et al., 2015). However, many clinically relevant pathogens have already developed resistance-mechanisms against many of these drugs thereby rendering antibiotic therapy of appropriate infections often ineffective (Meka and Gold, 2004; Chambers and Deleo, 2009; GBD 2019 Antimicrobial Resistance Collaborators, 2022a). Moreover, the rapid exchange of antibiotic resistance genes via horizontal gene transfer events, along with the large-scale usage of antimicrobials in hospitals and in the animal industry, continuously triggers the emergence of new drug-resistant and globally spreading bacterial clones, highlighting the desperate need for novel treatment options to fight infectious diseases in human or animal hosts (Chambers and Deleo, 2009; Nubel, 2016; Jian et al., 2021).

Antibiotic-resistant bacteria are frequently associated with local and life-threatening infections in both, hospital environments and in the general community. Of particular concern are Mycobacteria, certain Gram-negative as well as Gram-positive bacteria including *Staphylococcus aureus*, a notorious pathogen that colonizes approximately 30% of the human population (Lowy, 1998; Kuehnert et al., 2006; Lee et al., 2018). *S. aureus* causes skin and soft tissue infections and is a widespread cause of endocarditis, septic arthritis, osteomyelitis, bacteremia, and sepsis (Lowy, 1998; Fridkin et al., 2005; Klevens et al., 2007). Moreover, this microbe triggers toxic shock syndrome, food poisoning, ventilator-associated pneumonia, and associated infections of the respiratory tract (Lowy, 1998; Lee et al., 2018; Torres et al., 2021). Nonetheless, a hallmark of staphylococcal disease is the formation of suppurative abscesses, where *S. aureus* provokes inflammatory responses that attract neutrophils, macrophages, and other immune cells to the site of the infection (Lowy, 1998; Cheng et al., 2011; Spaan et al., 2013). Abscess formation is further accompanied by liquefaction necrosis, the release of purulent exudates into circulating body fluids, and several defensive host responses designed to limit staphylococcal replication and spread (Cheng et al., 2011). For example, staphylococcal invasion of host tissues and abscess formation includes deposition of structural fibrin clusters, which shield

healthy tissues from disseminating staphylococci (Cheng et al., 2011). Moreover, neutrophils combat *S. aureus* by powerful mechanisms which involve phagocytosis, generation of reactive oxygen species, and the formation of neutrophil extracellular traps (NETs) (Spaan et al., 2013). NETs represent an extracellular matrix composed of nuclear and mitochondrial DNA spiked with antimicrobial peptides, cell-specific proteases, and granular proteins that together ensnare and kill microbial invaders (Brinkmann et al., 2004). However, *S. aureus* rapidly evades NET-mediated killing due to the secretion of a potent nuclease (Nuc) capable of disrupting these structures (Berends et al., 2010; von Kockritz-Blickwede and Winstel, 2022). Intriguingly, Nuc-mediated degradation of NETs leads to the release of deoxyribonucleoside monophosphates that can be converted by the staphylococcal cell surface protein AdsA (adenosine synthase A) into death-effector deoxyribonucleosides (Thammavongsa et al., 2013; Tantawy et al., 2022). Notably, AdsA-derived death-effector deoxyribonucleosides such as deoxyadenosine (dAdo) and deoxyguanosine (dGuo) display toxigenic properties and contribute to immune cell death during acute and persistent *S. aureus* infections (Thammavongsa et al., 2013; Winstel et al., 2019; Tantawy et al., 2022). More precisely, dAdo and dGuo-triggered phagocyte cell death involves the uptake of dAdo and dGuo via human equilibrative nucleoside transporter 1 (hENT1), intracellular phosphorylation of dAdo and dGuo by adenosine kinase (ADK) and deoxycytidine kinase (dCK), and subsequent imbalanced expansion of intracellular dATP and dGTP pools which trigger caspase-3-dependent immune cell death (Winstel et al., 2018; Tantawy et al., 2022). Of note, genetic disruption of this metabolic cascade rendered macrophages resistant to AdsA-derived death-effector deoxyribonucleosides, leading to the accumulation of phagocytes within the deeper cavity of abscesses and accelerated clearance of staphylococci *in vivo* (Winstel et al., 2018; Winstel et al., 2019; Tantawy et al., 2022). Thus, elements of the mammalian purine salvage pathway represent attractive targets for the design of novel host-directed therapeutics that aim at boosting macrophage survival during acute and persistent *S. aureus* infections. In particular, pharmacological inhibition of dCK by small molecule inhibitors may terminate the intracellular conversion of *S. aureus*- and AdsA-derived death-effector deoxyribonucleosides into deoxyribonucleoside monophosphates and subsequent accumulation of apoptosis-triggering deoxyribonucleoside triphosphates in host phagocytes (Figure 1A). If so, *S. aureus*- and dAdo/dGuo-mediated macrophage cell death may efficiently be prevented thereby aiding in the clearance of staphylococci during abscess formation and persistent infections.

Here we provide proof of this concept by establishing a novel host-directed therapeutic strategy for prophylaxis and therapy of staphylococcal infectious diseases. Specifically, we show that the dCK-specific small molecule inhibitor (*R*)-DI-87 (((*R*)-2-((1-(2-(4-methoxy-3-(2-morpholinoethoxy)phenyl)-5-methylthiazol-4-yl)ethyl)thio)pyrimidine-4,6-diamine), an orally active, well-tolerated clinical-stage anti-cancer drug (Figure 1B) (Poddar et al., 2020), protects host phagocytes from staphylococcal death-effector deoxyribonucleoside-

128 mediated cytotoxicity and caspase-3-dependent cell death. Our results further suggest that administration of
129 (*R*)-DI-87 boosts macrophage survival during abscess formation and thus improves clinical outcomes in *S.*
130 *aureus*-infected laboratory animals.
131
132 **Results**
133 **(*R*)-DI-87-mediated blockade of mammalian dCK protects host immune cells from staphylococcal death-**
134 **effector deoxyribonucleosides.** To analyze whether pharmacological inhibition of mammalian dCK may
135 represent a suitable strategy to protect host phagocytes from staphylococcal death-effector
136 deoxyribonucleosides, we initially took advantage of various tissue culture model systems and pre-incubated
137 human U937 monocytes (U937) or U937-derived macrophages (U937 MΦ) with (*R*)-DI-87. Controls received
138 vehicle only. Following pre-incubation, U937 or U937 MΦ were exposed to dAdo or dGuo and analyzed for
139 viability rates 48 hours post-intoxication. Of note, (*R*)-DI-87-mediated inhibition of mammalian dCK in U937
140 or U937 MΦ efficiently prevented dAdo- or dGuo-induced cell death in a dose-dependent manner (Figure 2A-
141 D; supplementary Figure 1A-D). Moreover, these effects resembled the phenotype of dCK-deficient U937 or
142 U937 MΦ, which were found to be refractory to dAdo- or dGuo-mediated cytotoxicity (Figure 2A-D) (Winstel
143 et al., 2018; Tantawy et al., 2022). In addition, we observed that pre-treatment of primary human $CD14^+$
144 monocytes or human monocyte-derived macrophages (HMDMs) with (*R*)-DI-87 blocked dAdo- or dGuo-
145 triggered cytotoxicity suggesting that dCK inhibition may suppress the toxigenic properties of staphylococcal
146 death-effector deoxyribonucleosides (Figure 2E-H). To test this conjecture, we expressed a soluble and
147 affinity-tagged recombinant form of *S. aureus* AdsA (hereafter termed rAdsA) in *Escherichia coli*, which was
148 purified, released of its affinity tag, and subsequently used for cytotoxicity assays. Particularly, we incubated
149 rAdsA with either dAMP or dGMP according to a published protocol (Tantawy et al., 2022) and added the
150 resulting, dAdo- or dGuo-containing and filter-sterilized reaction products to U937 or U937 MΦ that received
151 (*R*)-DI-87 or were left untreated prior to intoxication. While enzymatic reactions that contained rAdsA and
152 purine deoxyribonucleoside monophosphates triggered cell death of human monocytes or macrophages in
153 this approach, (*R*)-DI-87-exposed cells were fully protected against the cytotoxic effect of dAdo and dGuo
154 further indicating that inhibition of mammalian dCK helps to neutralize AdsA-derived death-effector
155 deoxyribonucleosides (Figure 2I-J). In this regard, we also wondered whether these results can be
156 recapitulated by using live bacteria and took advantage of previously described methodologies
157 (Thammavongsa et al., 2013; Winstel et al., 2018; Winstel et al., 2019; Tantawy et al., 2022). More precisely,
158 we incubated wild-type *S. aureus* Newman or its *adsA* variant in the presence or absence purine
159 deoxyribonucleoside monophosphates (dAMP or dGMP) to obtain conditioned culture media, which were
160 filter-sterilized and added to vehicle- or (*R*)-DI-87-exposed human U937 macrophages. In line with earlier

161 studies (Thammavongsa et al., 2013; Winstel et al., 2018; Winstel et al., 2019; Tantawy et al., 2022),
162 macrophage killing required purine deoxyribonucleoside monophosphate-conditioned media and *adsA*-
163 proficient staphylococci as only wild-type *S. aureus* Newman and dAMP- or dGMP-supplemented media
164 triggered phagocyte cell death in this approach (Figure 2K-L). However, (*R*)-DI-87-exposed cells could not be
165 killed in these experiments supporting the idea that pharmacological inhibition of host dCK can shield
166 macrophages from *S. aureus*- and AdsA-driven cell death (Figure 2K-L). Collectively, these initial data
167 demonstrate that (*R*)-DI-87 is a suitable small molecule dCK inhibitor capable of preventing host immune cell
168 death induced by toxigenic products of the staphylococcal Nuc/AdsA pathway.
169
170 **(*R*)-DI-87 prevents death-effector deoxyribonucleoside-induced activation of apoptosis.** Earlier work
171 demonstrated that staphylococcal dAdo and dGuo target the mammalian purine salvage pathway to trigger
172 an exaggerated biogenesis of deoxyribonucleoside triphosphates, thereby igniting caspase-3-dependent host
173 immune cell death (Winstel et al., 2018; Winstel et al., 2019; Tantawy et al., 2022). Since the accumulation of
174 deoxyribonucleoside triphosphates and associated apoptotic signaling via cleavage of caspase-3 exclusively
175 occurs in dCK-proficient monocytes or macrophages upon intoxication with death-effector
176 deoxyribonucleosides such as dAdo (Winstel et al., 2018; Tantawy et al., 2022), it seemed plausible to us at
177 this stage that administration of (*R*)-DI-87 and inhibition of dCK may suppress dAdo- or dGuo-mediated
178 activation of the programmed cell death machinery. To test this hypothesis, U937 or U937 MΦ were pre-
179 incubated with (*R*)-DI-87, exposed to dAdo or dGuo, and used to generate cell extracts for evaluation of
180 caspase-3 activity by measuring the hydrolysis of the caspase-3-specific peptide substrate Ac-DEVD-pNA. As
181 expected, (*R*)-DI-87-treatment of U937 or U937 MΦ significantly decreased dAdo- or dGuo-mediated
182 activation of caspase-3 activity (Figure 3A-D). Since caspase-3 represents the key modulator of the apoptosis
183 signaling pathway, these data suggest that (*R*)-DI-87-mediated dCK inhibition selectively prevented dAdo- or
184 dGuo-mediated induction of apoptotic cell death in host immune cells (Figure 3A-D). To verify these results
185 further, cell extracts were also probed with a specific antibody capable of detecting the inactive pro-form and
186 cleaved (active) form of human caspase-3. In agreement with the enzymatic activity assay, (*R*)-DI-87-treatment
187 of U937 or U937 MΦ prevented caspase-3 activation (Figure 3E-F). Moreover, we exposed U937 phagocytes
188 to (*R*)-DI-87 and assessed dAdo- or dGuo-mediated activation of apoptotic signaling via immunofluorescence
189 microscopy. Microscopy-based analysis of (*R*)-DI-87- and death-effector deoxyribonucleoside-exposed
190 macrophages confirmed that (*R*)-DI-87 inhibited activation of programmed cell death and apoptosis as positive
191 signals for annexin-V/PI were strongly decreased in samples that have been exposed to the dCK inhibitor
192 (Figure 3G-H). Of note, similar findings were also obtained with primary HMDMs, suggesting that (*R*)-DI-87 is
193 a suitable agent to block death-effector deoxyribonucleoside-mediated induction of apoptosis in host

194 phagocytes (supplementary Figure 2). Together, these data indicate that administration of (*R*)-DI-87 and
195 associated inhibition of mammalian dCK prevents apoptotic cell death in phagocytes caused by *S. aureus* AdsA-
196 derived death-effector deoxyribonucleosides.
197
198 **Pharmacological inhibition of host dCK diminishes *S. aureus* abscess formation in a mouse model of**
199 **bloodstream infection.** To evaluate the therapeutic value of (*R*)-DI-87 in live animals, initial *in vivo*
200 experiments aimed at analyzing the safety of (*R*)-DI-87 in mice following continuous dCK inhibitor treatment.
201 Thus, cohorts of female C57BL/6 mice were treated from day 0 onwards with either vehicle (40% Captisol) or
202 (*R*)-DI-87 (75 mg/kg) via oral gavage in 12-hour intervals according to a published protocol (Chen et al., 2022a).
203 On day 16, peripheral blood was collected from both cohorts of mice and subjected to a FACS-based immuno-
204 phenotyping approach (Figure 4A). Continuous treatment of animals with (*R*)-DI-87 did not alter the immune
205 cell composition of peripheral blood (Figure 4A). Likewise, endpoint analysis (day 23) uncovered no
206 developmental errors or differences in lymphocyte development as immune cell profiles of spleen tissues
207 along with organ cellularity or mouse body weights were unaffected by (*R*)-DI-87 treatment (Figure 4B-D;
208 supplementary Figure 3). Further, administration of (*R*)-DI-87 to mice did not cause any other obvious
209 phenotype during this procedure but led to the accumulation of deoxycytidine, the natural substrate of dCK
210 (Reichard, 1988; Arner and Eriksson, 1995), in plasma suggesting that (*R*)-DI-87 not only represents a safe but
211 also highly selective inhibitor of host dCK (Figure 4E). Next, we sought to investigate whether (*R*)-DI-87-
212 mediated protection of mammalian phagocytes may represent a valuable strategy to prevent staphylococcal
213 diseases and tested the therapeutic efficacy of the compound in a mouse model of *S. aureus* bloodstream
214 infection. In this model, C57BL/6 mice were treated with (*R*)-DI-87 (75 mg/kg) or vehicle (40% Captisol) via oral
215 gavage every 12 hours and challenged with a single dose of 1.0 x 10^7 CFU *S. aureus* Newman, a human clinical
216 isolate (Duthie and Lorenz, 1952). Five days post-infection, mice were euthanized. Livers and kidneys were
217 dissected and analyzed for visible abscess lesions. Subsequently, tissue homogenates were prepared and
218 plated on agar plates to measure bacterial loads in infected organs. Notably, abscess numbers and bacterial
219 loads were significantly reduced in livers and kidneys in (*R*)-DI-87-treated animals as compared to control mice
220 validating (*R*)-DI-87 as a novel host-directed and anti-infective drug that protects against staphylococcal
221 abscess formation (Figure 4F-I). To test whether *S. aureus* exploits the activity of dCK along with the purine
222 salvage pathway during infection, cohorts of mice were also challenged with the *S. aureus* Newman *adsA*
223 mutant. (*R*)-DI-87-treated animals no longer displayed increased resistance to *S. aureus* infection (Figure 4F-
224 I). Moreover, infection with *S. aureus adsA*-deficient bacteria phenocopied (*R*)-DI-87-mediated inhibition of
225 dCK, in line with the concept that AdsA is required for establishing persistent infections in host tissues (Figure
226 4F-I). In light of these findings, infected organs were also fixed with formalin, embedded into paraffin, thin-

227 sectioned, and analyzed for histopathology. As expected, histopathological analysis of hematoxylin and eosin
228 (H&E)-stained liver or renal tissues revealed that wild-type *S. aureus* Newman formed structured abscesses in
229 vehicle-treated mice (Figure 4J). However, lesions obtained from (*R*)-DI-87-treated animals appeared smaller
230 in size and typically did not harbor a discernable organization of staphylococci, further demonstrating that
231 administration of (*R*)-DI-87 represents a medically valuable strategy to mitigate *S. aureus* abscess formation
232 (Figure 4J). Presumably, (*R*)-DI-87-treatment protects macrophages against AdsA-derived death-effector
233 deoxyribonucleosides and therefore enhances phagocyte survival during abscess formation as (*R*)-DI-87
234 neither improved the killing of *S. aureus* in human or mouse blood, nor it displayed antimicrobial activity
235 (supplementary Figure 4A-B; supplementary Table 1). Collectively, these data indicate that inhibition of
236 mammalian dCK by (*R*)-DI-87 attenuates *S. aureus* abscess formation and disease pathogenesis *in vivo*.
237
238 **(*R*)-DI-87-treatment amplifies macrophage infiltration into staphylococcal infectious foci.** Previous studies
239 revealed that macrophages with defects in the purine salvage pathway-apoptosis axis are refractory to
240 staphylococcal dAdo or dGuo (Winstel et al., 2018; Winstel et al., 2019; Tantawy et al., 2022). As a result,
241 death-effector deoxyribonucleoside-resistant tissue macrophages were found to accumulate within deep-
242 seated abscesses of *S. aureus*-challenged mice, a phenomenon that contributed to accelerated clearance of
243 staphylococci (Winstel et al., 2019). Thus, we hypothesized that pharmacological inhibition of host dCK might
244 augment phagocyte infiltration into *S. aureus*-derived abscesses, thereby explaining reduced bacterial burdens
245 in (*R*)-DI-87-treated laboratory animals. To pursue this possibility, we established an immunofluorescence
246 microscopy-based approach to detect macrophages in liver or renal tissues of *S. aureus* Newman wild type-
247 infected C57BL/6 mice that were treated with (*R*)-DI-87 or vehicle only. As expected, immunofluorescence
248 staining of tissue abscesses obtained from vehicle-treated animals revealed that F4/80-positive macrophages
249 resided at the periphery of infectious foci (Figure 5A-D). On the contrary, lesions derived from mice that
250 received (*R*)-DI-87 differed as they contained infiltrates of F4/80-positive macrophages within the neutrophil
251 cuff, suggesting that (*R*)-DI-87-mediated inhibition of host dCK terminates macrophage exclusion from
252 staphylococcal infectious foci (Figure 5E-H). To further delineate whether these results correlate with AdsA
253 and staphylococcal death-effector deoxyribonucleoside-mediated manipulation of host dCK in phagocytes,
254 tissues of *S. aureus* Newman *adsA* mutant-infected mice, which received either (*R*)-DI-87 or vehicle, were also
255 examined via immunofluorescence microscopy and analyzed for the presence of F4/80-positive macrophages.
256 Of note, *adsA* mutant-derived tissue lesions were also characterized by increased infiltration rates of F4/80-
257 positive phagocytes, irrespectively of whether animals were treated with (*R*)-DI-87 or vehicle during the course
258 of the infection (Figure 5I-P). Thus, (*R*)-DI-87-mediated blockade of host dCK phenocopied the *adsA* mutation
259 in *S. aureus*. Lastly, (*R*)-DI-87- or vehicle-treated bone marrow-derived macrophages (BMDMs) that were

260 isolated from female animals were analyzed for survival rates upon exposure to dAdo or dGuo. Compared to
261 vehicle-treated cells, which were susceptible to death-effector deoxyribonucleosides, BMDMs exposed to (*R*)-
262 DI-87 displayed increased resistance toward dAdo and dGuo presumably explaining their abundance in
263 infectious foci obtained from wild-type *S. aureus* Newman-challenged and dCK inhibitor-treated mice (Figure
264 5Q-R). Similar findings were also obtained for male animal-derived BMDMs suggesting that sex might not
265 impact the efficacy of (*R*)-DI-87 in laboratory animals (supplementary Figure 5A-B). In summary, these data
266 suggest that (*R*)-DI-87-treatment protects macrophages from staphylococcal death-effector
267 deoxyribonucleosides and therefore boosts their infiltration into persistent abscesses in organ tissues (Figure
268 6).
269
270 **Discussion**
271 Bacterial infectious diseases are typically treated with specific or broad-spectrum antibiotics. However, many
272 microbial pathogens have developed resistance mechanisms against these drugs and other antimicrobial
273 agents either via mutational changes within the drug target or by importing resistance genes from other
274 bacteria (Klevens et al., 2008; Yaw et al., 2014; Nubel, 2016; Jian et al., 2021; GBD 2019 Antimicrobial
275 Resistance Collaborators, 2022a). Accordingly, infections by multidrug-resistant microbes are frequently
276 associated with failure of therapy and increased mortality in both, industrialized and developing countries
277 around the world (Klevens et al., 2008; Yaw et al., 2014; GBD 2019 Antimicrobial Resistance Collaborators,
278 2022a; b). Each year, several million people die due to infections caused by drug-resistant bacteria such as
279 *Mycobacterium tuberculosis*, *E. coli*, or *S. aureus* underscoring the very urgent need of new therapeutics and
280 anti-infective compounds against which bacteria cannot develop resistance (Pai et al., 2016; GBD 2019
281 Antimicrobial Resistance Collaborators, 2022a; b).
282 Host-directed therapy is an emerging therapeutic concept that eliminates the possibility of drug
283 resistance development in microbial pathogens (Kaufmann et al., 2018). This innovative approach aims at
284 targeting specific host determinants and signaling cascades bacterial or other pathogenic microorganisms may
285 attack or exploit to establish acute and persistent infections (Kaufmann et al., 2018). Overall, this strategy
286 seeks to ameliorate host immunity, immune cell survival, and immunopathology, as well as pathogen control
287 without interfering with microbial replication, growth, or metabolism (Kaufmann et al., 2018). By applying this
288 concept along with a drug-repurposing approach, we here report that administration of (*R*)-DI-87, a soluble,
289 orally active, and high-affinity inhibitor of host dCK (Poddar et al., 2020), reduces *S. aureus* abscess formation
290 in a mouse model of bloodstream infection. In particular, we show that (*R*)-DI-87-mediated blockade of host
291 dCK prevents staphylococcal death-effector deoxyribonucleoside-triggered apoptotic cell death in phagocytes

292 of human and animal origin. Accordingly, oral administration of (*R*)-DI-87 in mice rendered host phagocytes
293 refractory to AdsA-derived dAdo and dGuo thereby leading to an accumulation of *S. aureus*-eliminating
294 macrophages within deeper cavities of infectious foci along with accelerated phagocytic clearance of
295 staphylococci. Since dCK is a rate-limiting enzyme of the nucleoside salvage pathway that catalyzes the
296 intracellular conversion of deoxyribonucleosides into deoxyribonucleoside monophosphates (Arner and
297 Eriksson, 1995), (*R*)-DI-87-mediated inhibition of dCK most likely suppresses an uncontrolled biogenesis of
298 deoxyribonucleoside di- and triphosphates that may trigger replication errors and apoptosis in host cells.
299 Consistent with this model, earlier work suggested that dCK deficiency in phagocytes or other cells such as
300 lymphoblasts prevents an overload of intracellular deoxyribonucleoside triphosphates upon exposure to
301 death-effector deoxyribonucleosides (Gudas et al., 1978; Winstel et al., 2018). Thus, inhibition of host dCK
302 represents an attractive host-directed therapeutic intervention strategy that terminates a refined immuno-
303 evasive maneuver *S. aureus* has evolved to establish persistent infections in mammalian hosts. The
304 technological advantage of this therapeutic approach, beyond the clinical importance and long-term economic
305 benefits for the medical-therapeutic sector, is undoubtedly the exploitation of an already existing, highly
306 selective, and clinical-stage compound that can easily be administered to dampen metastatic abscess
307 formation in organs upon staphylococcal bloodstream infection. In particular, (*R*)-DI-87 does not exhibit
308 detrimental side effects as (*R*)-DI-87-exposed laboratory animals neither lost weight during long-term
309 treatment nor displayed any other adverse effects that may negatively affect host immune responses.
310 Specifically, the immune cell composition profile of mice that received (*R*)-DI-87 was not altered when
311 compared to mice that received the vehicle control. This suggests that patrolling neutrophils known to play a
312 significant role during staphylococcal infections (Spaan et al., 2013) along with other crucial elements of the
313 host immune system are fully functional in (*R*)-DI-87-treated hosts, thereby offering tremendous opportunities
314 to improve infection outcomes in hospitalized or critically ill patients. Further, usage of (*R*)-DI-87 represents a
315 host-directed and anti-infective therapeutic approach to which *S. aureus* and other multidrug-resistant
316 bacteria cannot develop resistance mechanisms. In this regard, we note that many other medically highly
317 relevant bacterial pathogens including streptococci, *Bacillus anthracis*, and multidrug-resistant *Staphylococcus*
318 *pseudintermedius* synthesize effector-nucleosides in order to modulate host immune cell responses
319 (Thammavongsa et al., 2009; Liu et al., 2014; Zheng et al., 2015; Ma et al., 2017; Dai et al., 2018; Bunsow et
320 al., 2021). Thus, (*R*)-DI-87-mediated inhibition of dCK may also help to protect host cells from apoptotic cell
321 death or other adverse effects during other bacterial diseases in human or animal hosts. Even polymicrobial
322 infections caused by various microbial pathogens and other infectious agents that manipulate the purine
323 salvage pathway-apoptosis axis during infection can eventually be prevented, attenuated, or treated by using
324 (*R*)-DI-87. Nevertheless, administration of (*R*)-DI-87 did not completely abolish disease development and

325 abscess formation during sub-lethal bloodstream infection in mice. Thus, double-pronged therapies which
326 cover the usage of (*R*)-DI-87 combined with antibiotics, various anti-infective agents, or monoclonal
327 antibodies, some of which are known to neutralize predominant staphylococcal virulence determinants,
328 including secreted toxins (Ragle and Bubeck Wardenburg, 2009; Hua et al., 2014; Thomsen et al., 2017),
329 protein A (Kim et al., 2012; Chen et al., 2022b), and specific surface antigens (Bennett et al., 2019; de Vor et
330 al., 2022) along with usage of other host-directed therapeutics that impede *S. aureus* disease pathogenesis
331 (Bravo-Santano et al., 2019; Alphonse et al., 2021), may essentially improve disease progression during
332 staphylococcal infections. Ultimately, combinatorial therapies that involve usage of (*R*)-DI-87 may even help
333 to enhance outcomes of life-threatening septicemia or other fatal bacterial infectious diseases and should
334 therefore be considered for pre-clinical tests in animal models.

335 Overall, (*R*)-DI-87-mediated inhibition of dCK is a novel host-directed therapeutic concept to mitigate
336 staphylococcal abscess formation in organ tissues upon bloodstream infection. Since (*R*)-DI-87 is extremely
337 well tolerated in humans (personal communication; Kenneth A. Schultz, Trethera Corporation, Los Angeles,
338 CA, USA) and currently being investigated in phase I clinical trials for the treatment of non-communicable
339 diseases, including cancer and multiple sclerosis (Poddar et al., 2020; Chen et al., 2022a), this compound
340 already meets the requirements for a prompt launch of clinical studies in individuals that suffer local or
341 invasive staphylococcal infections. Optimization of (*R*)-DI-87 or any medically acceptable derivatives thereof
342 may further accelerate this process and concurrently could also aid in the design of pre-exposure prophylactic
343 agents for hospitalized or high-risk patients, with the primary aim to enhance infection control and public
344 health.

345

346 **Materials und methods**

347 **Bacterial strains and growth conditions.** All bacterial strains used in this study are listed in the *Supplementary*
348 *Materials* (supplementary Table 2). Bacteria were grown in tryptic soy broth (TSB), Mueller-Hinton broth
349 (MHB), or lysogeny broth (LB) at permissive temperatures. Media were supplemented with appropriate
350 antibiotics (ampicillin 100 µg/ml).

351 **Cell lines and tissue culture.** U937 cells were obtained from American Type Culture Collection (ATCC) and
352 grown in Roswell Park Memorial Institute (RPMI) 1640 medium (Gibco) supplemented with 10% heat-
353 inactivated fetal bovine serum (hi-FBS) according to the manufacturer's instructions. All mammalian cell lines
354 were grown at 37°C under 5% CO_2. Cell lines used in this study are listed in the *Supplementary Materials*
355 (supplementary Table 3).

356 **Isolation of human primary cells.** Peripheral blood mononuclear cells (PBMCs) were isolated from heparinized
357 blood by density gradient centrifugation on Pancoll (PAN Biotech) according to standard laboratory protocols.
358 Next, human primary monocytes were isolated from PBMCs by using magnetic nanobeads and the MojoSort™
359 Human CD14 Selection Kit (BioLegend) as described earlier (Tantawy et al., 2022). Subsequently, purified
360 primary CD14-positive ($CD14^+$) monocytes were resuspended in RPMI 1640 medium containing 10% hi-FBS
361 and 1% penicillin-streptomycin and used for cytotoxicity assays. Alternatively, purified $CD14^+$ monocytes were
362 differentiated into human monocyte-derived macrophages (HMDMs) in the same medium supplemented with
363 50 ng/ml of human macrophage colony stimulating factor (hM-CSF; Genscript). HMDMs were used at day 7
364 post-differentiation for cytotoxicity experiments.

365 **Isolation of murine bone marrow-derived macrophages.** Bone marrow-derived macrophages (BMDMs) were
366 isolated from C57BL/6 mice as previously described (Tantawy et al., 2022). In brief, mice were euthanized to
367 remove the femur and tibia which were sterilized by using 70% ethanol. Bones were then washed with sterile
368 phosphate-buffered saline (PBS). Next, the bone ends were removed and the bone marrow was flushed out
369 by using RPMI 1640 containing 10% hi-FBS and 1% penicillin-streptomycin. Following a resuspension step, cells
370 were passed through a nylon cell strainer (40 µm) to remove unwanted tissue and cellular debris.
371 Subsequently, cells were centrifuged (10 min, 200 x g, 4°C), resuspended in red blood cell (RBC) lysis buffer
372 (Roche), and incubated for 5 min at room temperature to lyse RBC. Cells were centrifuged once more,
373 resuspended in BMDM medium (RPMI 1640 containing 10% hi-FBS, 1% penicillin-streptomycin, and 50 ng/ml
374 of mouse macrophage colony-stimulating factor (Genscript)), and seeded into tissue culture-treated dishes to
375 deplete bone marrow cells from fibroblasts. At day 1 post-extraction, suspension bone marrow cells were
376 collected via centrifugation, adjusted to 6.0 x 10^5 cells/ml in BMDM medium, and re-seeded into
377 bacteriological dishes. At day 4 post-extraction, cells were incubated with an additional 10 ml of BMDM
378 medium. BMDMs were used at day 7 post-extraction for cytotoxicity experiments.

379 **Protein purification.** Purification of recombinant *S. aureus* AdsA was performed as described elsewhere
380 (Thammavongsa et al., 2009; Tantawy et al., 2022). Briefly, a glutathione S-transferase (GST)-tagged and
381 recombinant version of *S. aureus* AdsA (rAdsA) was expressed in *E. coli* BL21 using the pGEX-2T plasmid system
382 (GE Healthcare) and purified via glutathione S-transferase affinity chromatography (Thammavongsa et al.,
383 2009; Tantawy et al., 2022). Next, the N-terminal GST tag was removed by using thrombin which was
384 immediately cleared from the protein sample via benzamidine sepharose beads according to the
385 manufacturer's instructions (GE Healthcare). Purified rAdsA was analyzed by a Coomassie-stained SDS-PAGE
386 following standard laboratory protocols.

387 **Cytotoxicity assays.** To evaluate the protective role of (*R*)-DI-87 during death-effector deoxyribonucleoside-
388 induced cytotoxicity, 2.0 x 10^5 U937 monocyte-like cells (U937) per well were seeded in a 24-well plate and
389 pre-incubated for 2 h at 37°C under 5% CO_2 in RPMI 1640 medium containing 10% hi-FBS and 1 µM of (*R*)-DI-
390 87. Control wells received vehicle only. Alternatively, 4.0 × 10^5 U937 cells per well were seeded in a 24-well
391 plate and incubated for 48 h at 37°C under 5% CO_2 in RPMI 1640 growth medium that contained 160 nM
392 phorbol 12-myristate 13-acetate (PMA). Resulting U937-derived macrophages (U937 MΦ) were washed and
393 further incubated in RPMI 1640 growth medium lacking PMA (24 h). Similarly, 3.5 x 10^5 BMDMs per well were
394 seeded in 24-well plates and incubated for 24 h at 37°C under 5% CO_2 in corresponding growth media. Next,
395 U937 MΦ or BMDMs were washed once and pre-incubated for 2 h at 37°C under 5% CO_2 in appropriate growth
396 media supplemented with 1 µM of (*R*)-DI-87. Control wells received vehicle only. Following pre-incubation
397 with (*R*)-DI-87, U937, U937 MΦ, or BMDMs were exposed to various concentrations of either dAdo or dGuo
398 (100 µM for U937; 200 µM for U937 MΦ or BMDMs) and incubated for 48 h at 37°C under 5% CO_2 in RPMI
399 1640 growth medium. Cells were collected via centrifugation (U937) or a detachment-centrifugation step
400 using trypsin-EDTA (U937 MΦ) or accutase (BMDMs) solution. Dead cells were stained with trypan blue and
401 counted by using a microscope to calculate killing efficiency. To analyze the protective effect of (*R*)-DI-87 in
402 primary human cells, 2.0 x 10^5 $CD14^+$ monocytes or HMDMs per well were seeded in multi-well plates and pre-
403 incubated for 2 h at 37°C under 5% CO_2 in RPMI 1640 medium containing 10% hi-FBS and 1 µM of (*R*)-DI-87.
404 Control wells received vehicle only. Subsequently, cells were intoxicated by using various concentrations of
405 either dAdo or dGuo (100 µM for $CD14^+$ monocytes; 200 µM for HMDMs) and incubated in appropriate growth
406 media for 48 h at 37°C under 5% CO_2. Cells were collected via centrifugation ($CD14^+$ monocytes) or a
407 detachment-centrifugation step (HMDMs) using trypsin-EDTA solution. Viability of cells was determined via
408 trypan blue staining and microscopy as described above. To block the cytotoxic effect of AdsA-derived death-
409 effector deoxyribonucleosides by using (*R*)-DI-87, rAdsA (1.25 µg/µl) was incubated for 16 h at 37°C in a
410 reaction buffer (30 mM Tris-HCl, pH 7.5; 1.5 mM $MgCl_2$; 1.5 mM $MnCl_2$) supplemented with either dAMP or
411 dGMP (1.19 mM each) according to a published protocol (Tantawy et al., 2022). Controls included reactions
412 that lacked deoxyribonucleoside monophosphates or rAdsA. Following incubation, all reaction products were
413 filter-sterilized and added to U937 MΦ which were pre-incubated with vehicle or 1 µM (*R*)-DI-87 for 2 h prior
414 to intoxication. Next, cells were incubated at 37°C under 5% CO_2 for 48 h, collected, and analyzed via trypan
415 blue staining and microscopy as described above. *S. aureus*-driven cell death was analyzed based on previously
416 described approaches (Thammavongsa et al., 2013; Winstel et al., 2018; Winstel et al., 2019; Tantawy et al.,
417 2022). In brief, the *S. aureus* Newman strain panel was incubated overnight at 37°C in TSB, diluted in fresh TSB
418 medium, and grown at 37°C to 1.5 x 10^8 CFU/ml. Next, staphylococci were pelleted, washed twice in sterile
419 wash buffer (50 mM Tris-HCl; pH 7.5), and adjusted to 3.2 x 10^8 CFU/ml. 8.0 x 10^7 CFU were incubated in a

420 dAMP- or dGMP-containing (final conc. 5 mM) reaction buffer (30 mM Tris-HCl, pH 7.5; 2 mM $MgCl_2$) for 90
421 min at 37°C. Controls lacked bacteria, dAMP, dGMP, or involved the *S. aureus adsA* mutant, which cannot
422 synthesize dAdo and dGuo. Following incubation, bacteria were removed from the sample by a brief
423 centrifugation-filtration step. 300 µl of the resulting and filter-sterilized supernatants were mixed with 700 µl
424 of RPMI growth medium and incubated with vehicle- or (*R*)-DI-87-exposed (1 µM) U937-derived macrophages
425 for 24 h at 37°C under 5% CO_2. Finally, cells were detached, collected, and stained with trypan blue as
426 described above to quantify killed phagocytes.

427 **Assessment of caspase-3-activity.** Caspase-3 activity was analyzed using a colorimetric caspase-3 detection
428 kit (Sigma) and a published protocol (Winstel et al., 2018; Tantawy et al., 2022). Briefly, U937 cells or U937
429 MΦ along with appropriate controls were pre-incubated for 2 h at 37°C under 5% CO_2 in RPMI 1640 medium
430 containing 10% hi-FBS and 1 µM of (*R*)-DI-87. Controls received vehicle only. Subsequently, cells were exposed
431 to various concentrations of either dAdo or dGuo (100 µM for U937; 200 µM for U937 MΦ) and incubated for
432 24 h at 37°C under 5% CO_2 in RPMI 1640 growth medium. Cells were collected via centrifugation (U937) or a
433 detachment-centrifugation step (U937 MΦ) using trypsin-EDTA solution and washed once in PBS. Next, 1.0 x
434 10^7 cells were lysed in pre-chilled lysis buffer (Sigma kit) for 20 min. This step was performed on ice. Resulting
435 lysates were centrifuged at 4°C (18,000 × g for 10 min) to obtain cell- and debris-free supernatants which were
436 incubated with the caspase-3 substrate Ac-DEVD-pNA according to the manufacturer's instructions. Caspase-
437 3 activity was determined based on the amount of released pNA that can be detected at 405 nm.

438 **Immunoblotting.** Immunoblotting was performed as described elsewhere (Tantawy et al., 2022). In short,
439 U937 or U937 MΦ and appropriate controls were pre-incubated for 2 h at 37°C under 5% CO_2 in RPMI 1640
440 medium containing 10% hi-FBS and 1 µM of (*R*)-DI-87. Controls received vehicle only. Next, cells were treated
441 with dAdo or dGuo (100 µM for U937; 200 µM for U937 MΦ), incubated for 24 h at 37°C under 5% CO_2 in RPMI
442 1640 growth medium, and collected via centrifugation (U937) or a detachment-centrifugation step (U937 MΦ)
443 using trypsin-EDTA solution. Cells were washed once in PBS. 1.0 x 10^7 cells were lysed on ice in pre-chilled lysis
444 buffer (50 mM HEPES, pH 7.4; 5 mM CHAPS; 5 mM DTT) for 20 min. Resulting lysates were centrifuged at 4°C
445 (18,000 × g for 10 min) to obtain cell- and debris-free supernatants which were mixed with sodium dodecyl
446 sulfate-polyacrylamide gel (SDS-PAGE) loading buffer. Samples were boiled for 10 min at 95°C. Proteins were
447 separated via SDS-PAGE (12%) and transferred onto PVDF membranes for immunoblot analysis with the
448 following rabbit primary antibodies: α-Caspase-3 (α-CASP3, 9662, Cell Signaling) and α-GAPDH (ab181602,
449 Abcam, loading control). Immunoreactive signals were revealed with a secondary antibody conjugated to
450 horseradish peroxidase (α-rabbit IgG, 7074, Cell Signaling). Horseradish peroxidase activity was detected with
451 enhanced chemiluminescent (ECL) substrate (Thermo Fisher).

452 **FITC-annexin-V/PI staining.** FITC-annexin-V/PI staining of U937 MΦ or HMDMs exposed to 1 µM (*R*)-DI-87 and
453 death-effector deoxyribonucleosides (200 µM dAdo or dGuo; 24 h at 37°C) along with appropriate controls
454 was performed by using FITC-annexin-V Apoptosis Detection Kit I (BD Biosciences) according to the
455 manufacturer's instructions. Stained cells were analyzed via immunofluorescence microscopy according to
456 standard laboratory protocols.

457 **Determination of the minimal inhibitory concentration (MIC).** The MIC of (*R*)-DI-87 was determined in 96-
458 well plates by using the microdilution method and Mueller-Hinton broth according to standard laboratory
459 protocols. Wells containing varying concentrations of (*R*)-DI-87 or vehicle were inoculated with 10^5 CFU/ml of
460 wild-type *S. aureus* Newman or its *adsA* mutant and incubated for 24 h at 37°C under continuous shaking. The
461 MIC was defined as the lowest concentration of compound at which no visible growth was detected.

462 **Bacterial survival in blood.** Bacterial survival in mouse or human blood was analyzed as described before
463 (Thammavongsa et al., 2009). In brief, fresh overnight cultures of *S. aureus* Newman wild type or its *adsA*
464 mutant were diluted into fresh TSB medium and grown at 37°C to an OD of 1.0. Bacteria were washed twice
465 in sterile PBS and adjusted in PBS to a final density of 1.0 x 10^8 CFU/ml. Next, freshly drawn mouse or human
466 blood anticoagulated with heparin was incubated in the presence or absence of 1 µM (*R*)-DI-87 for 60 min
467 (37°C) with *S. aureus* Newman wild type or its *adsA* mutant using a bacterial dose of 1.0 x 10^6 CFU/ml (murine
468 blood) or 1.0 x 10^7 CFU/ml (human blood). Samples without (*R*)-DI-87 treatment received the vehicle.
469 Following incubation, blood samples were mixed in a 1:1 ratio with sterile lysis buffer (PBS containing 1.0%
470 saponin) and incubated for 10 min at 37°C to lyse eukaryotic cells. Subsequently, serial dilutions were prepared
471 and plated onto TSA plates to determine bacterial survival rates.

472 **Animal infection model.** C57BL/6 mice were purchased from Janvier Laboratories and kept under specific
473 pathogen-free conditions in our central mouse facility (TWINCORE, Center for Experimental and Clinical
474 Infection Research, Hannover, Germany). Mice received (*R*)-DI-87 (75 mg/kg) or vehicle (40% Captisol) via oral
475 gavage at the day of the infection, separated by 12-hour intervals over a 5-day observation period. Timing of
476 intervention therapy was initiated six hours before systemic challenge. For infection experiments, TSB
477 overnight cultures of wild-type *S. aureus* Newman or its *adsA* mutant were diluted 1:100 in TSB and grown to
478 an optical density (600 nm) of 0.5. Bacteria were then centrifuged (10 min, RT, 8,000 × g), washed twice in
479 sterile PBS, and adjusted to 10^8 CFU/ml. One hundred microliters of the bacterial suspension (10^7 CFU) were
480 administered intravenously (lateral tail vein) into 6- to 8-weeks-old female C57BL/6 mice. Five days post-
481 infection, animals were euthanized. Organs were dissected, examined for surface abscesses, and homogenized
482 in sterile PBS supplemented with 0.1% Triton X-100. Serial dilutions were prepared and plated onto TSA plates

483 to determine bacterial loads. For histopathology, dissected organs were fixed in 10% Formalin (Sigma),
484 embedded into paraffin, thin-sectioned, and stained with hematoxylin and eosin (H&E). Stained tissues were
485 examined by microscopy according to standard laboratory protocols.

486 **Immunofluorescence staining.** To detect macrophages in *S. aureus*-infected tissues, formalin-fixed and
487 paraffin-embedded organs were thin-sectioned, deparaffinized, and rehydrated. After heat-induced antigen
488 retrieval in 10 mM sodium citrate buffer (pH 6.0), non-specific antibody binding was blocked by adding 2%
489 normal goat serum. Immunofluorescence staining was carried out by using an antibody against F4/80-positive
490 macrophages (α-F4/80, 70076, Cell Signaling), followed by a fluorescently-labelled secondary antibody
491 (Alexa546, Invitrogen). Stained tissues were examined by using a Zeiss Apotome 2 microscope (Zeiss).

492 **Safety assessment of (*R*)-DI-87.** To assess the therapeutic value and safety of (*R*)-DI-87, cohorts of female
493 C57BL/6 mice were treated with (*R*)-DI-87 (75 mg/kg) or vehicle (40% Captisol) via oral gavage in 12-hour
494 intervals over the course of 23 days. On day 16, 100 µl peripheral blood was collected in lithium heparin-
495 coated tubes via retro-orbital bleeding using heparin-coated capillary tubes. Subsequently, blood samples
496 were incubated with 5 ml of ACK lysis buffer at room temperature for 5 min, quenched with 5 ml of FACS
497 buffer (5% FBS in PBS), and centrifuged at 4°C (4 min). This process was repeated and cells were subsequently
498 stained with the following fluorochrome-conjugated anti-mouse antibodies diluted 1:100 in 100 µl of FACS
499 buffer for 20 min at 4°C: α-B220-PerCP/Cy5.5 (103236, BioLegend), α-CD4-BV711 (100550, BioLegend), α-
500 CD8α-PE (100708, BioLegend), α-CD11c-PE/Dazzle594 (117347, BioLegend), α-CD11b-FITC (101206,
501 BioLegend), α-GR1-APC (108412, BioLegend); α-CD16/32 (FC block; 101319; BioLegend). Following incubation,
502 cells were centrifuged and washed twice using FACS buffer. Cells were resuspended in FACS buffer and
503 analyzed using a BD LSRII flow cytometer and the FlowJo software package. During the (*R*)-DI-87 or vehicle
504 treatment procedure, mice were also regularly monitored and weighed to assess the overall health status. On
505 day 23, an endpoint analysis was carried out to analyze the immune cell profile and cellularity of spleen and
506 thymus tissues as described elsewhere (Abt et al., 2022). Lastly, blood was collected from all cohorts of animals
507 for the analysis of the deoxycytidine (dC) content in mouse plasma to evaluate the dCK-inhibitory capacity of
508 (*R*)-DI-87 (see below).

509 **LC-MS/MS-MRM analysis of plasma nucleoside levels**. LC-MS/MS-MRM analysis of plasma nucleoside levels
510 was performed as previously described (Le et al., 2017). For the analysis of plasma deoxycytidine levels, blood
511 was collected from mice using a heparin-coated capillary tube by the retro-orbital technique and transferred
512 to a lithium-heparin coated tube (Fisher Cat#13-680-62) on ice. Samples were centrifuged at 450 x g for 5
513 minutes at 4°C and the plasma supernatant was stored at -80°C. For metabolite extraction, 20 µL of plasma

514 was mixed with 80 µL of 100% MeOH containing stable isotope-labeled nucleoside internal standard (0.5 µM
515 [U-^{15}N/^{13}C]dC; Silantes Cat#124603802). MeOH-extracted samples were incubated at -80°C for 24 hours,
516 centrifuged at 12,000 x g for 5 minutes at 4°C, and the cleared supernatant was transferred to an HPLC injector
517 vial for analysis. 5 µL of the sample was injected onto a porous graphitic carbon column (Thermo Fisher
518 Scientific Hypercarb, 100 x 2.1 mm, 5 µm particle size) equilibrated in solvent A (0.1% formic acid in MiliQ-
519 purified/LC-Pak treated H_2O) and eluted (700 µL/min) with an increasing concentration of solvent B (0.1%
520 formic acid in acetonitrile) using min/%B/flow rates (µL/min) as follows: 0/2/700, 3/80/700, 4/80/700,
521 4.5/2/700, 7/2/700. The effluent from the column was directed to an Agilent Jet Stream ion source connected
522 to a triple quadrupole mass spectrometer (Agilent 6460) operating in the multiple reaction monitoring (MRM)
523 mode using previously optimized settings. The peak areas for each target molecule (precursor→fragment ion
524 transitions) at predetermined retention times were recorded using Agilent MassHunter software. Peak areas
525 were normalized to nucleoside internal standard signals. An external standard curve was applied to determine
526 nucleoside concentrations. Experimental and standard samples were processed together to minimize
527 variation.

528 **Ethics statement.** All animal experiments were conducted in accordance with the local animal welfare
529 regulations reviewed by the institutional review board and the Niedersächsisches Landesamt für
530 Verbraucherschutz und Lebensmittelsicherheit (LAVES) under the permission number 33.19-42502-04-
531 21/3696. Scientific use of animals (murine blood samples; isolation of BMDMs) was further carried out under
532 approved animal care and use protocols which are granted by the state veterinary authorities and overseen
533 by the internal animal care and use committee (IACUC). Animal studies required to assess the safety of (*R*)-DI-
534 87 in mice were approved by the UCLA Animal Research Committee (ARC). Human blood samples were
535 obtained from adult, consenting healthy donors. Informed consent forms were obtained from all participants.
536 These studies were reviewed and approved by the medical ethics committee of Hannover Medical School
537 (Hannover, Germany) under the permission number 8831_BO_K_2019.

538 **Synthesis and preparation of (*R*)-DI-87.** (*R*)-DI-87 ((((*R*)-2-((1-(2-(4-methoxy-3-(2-morpholinoethoxy)phenyl)-
539 5-methylthiazol-4-yl)ethyl)thio)pyrimidine-4,6-diamine) was synthesized as described before (Poddar et al.,
540 2020). For experiments, (*R*)-DI-87 was either dissolved in Dimethyl sulfoxide (*in vitro* experiments) or in an
541 aqueous solution containing 40% Captisol (CyDex Pharmaceuticals, Inc.) (*in vivo* experiments).

542 **Statistical analysis.** Statistical analysis was performed by using GraphPad Prism (GraphPad Software, Inc., La
543 Jolla, USA). Statistically significant differences were calculated by using statistical methods as indicated. *P*
544 values < 0.05 were considered significant.

Data availability. All data supporting the findings of this study are available within the article and its supplementary material. All other data are available from the corresponding author upon reasonable request.

Acknowledgments

We thank all laboratory members for helpful discussion. We are grateful for support from the German Research Foundation (award WI4582/2-1 to V.W., project number 449712894). E.R.A. is supported by UCLA Tumor Immunology Training Grant T32CA009120. This work was supported by National Institutes of Health grants to C.G.R. (1R01CA25052901A1 and 1R01CA260678-01).

Author contributions

Volker Winstel: Conceptualization; data curation; investigation; methodology; formal analysis; supervision; funding acquisition; writing – original draft; writing – review and editing; visualization; project administration. Evan R. Abt: Conceptualization; data curation; investigation; methodology; formal analysis; writing – review and editing. Thuc M. Le: Conceptualization; data curation; investigation; methodology; formal analysis; writing – review and editing. Caius G. Radu: Conceptualization; investigation; methodology; formal analysis; resources; funding acquisition; writing – review and editing.

Conflict of interest

C.G.R. is a co-inventor of the dCK inhibitor used in this study. This intellectual property has been patented by the University of California and optioned to Trethera Corporation, a company that C.G.R. owns equity in. V.W., E.R.A., and C.G.R. are inventors in a patent application covering the use of dCK inhibitors as a treatment for bacterial infectious diseases. T.M.L. declares no conflict of interest.

578 **References**

579 Abt ER, Rashid K, Le TM, Li S, Lee HR, Lok V, Li L, Creech AL, Labora AN, Mandl HK, Lam AK, Cho A, Rezek V, Wu
580 N, Abril-Rodriguez G, Rosser EW, Mittelman SD, Hugo W, Mehrling T, Bantia S, et al. (2022). Purine
581 nucleoside phosphorylase enables dual metabolic checkpoints that prevent T cell immunodeficiency
582 and TLR7-associated autoimmunity. *J Clin Invest* 132(16). doi: 10.1172/JCI160852.
583 Alphonse MP, Rubens JH, Ortines RV, Orlando NA, Patel AM, Dikeman D, Wang Y, Vuong I, Joyce DP, Zhang J,
584 Mumtaz M, Liu H, Liu Q, Youn C, Patrick GJ, Ravipati A, Miller RJ, Archer NK, and Miller LS (2021). Pan-
585 caspase inhibition as a potential host-directed immunotherapy against MRSA and other bacterial skin
586 infections. *Sci Transl Med* 13(601). doi: 10.1126/scitranslmed.abe9887.
587 Arner ES, and Eriksson S (1995). Mammalian deoxyribonucleoside kinases. *Pharmacol Ther* 67(2)**,** 155-186. doi:
588 10.1016/0163-7258(95)00015-9.
589 Bennett MR, Bombardi RG, Kose N, Parrish EH, Nagel MB, Petit RA, Read TD, Schey KL, Thomsen IP, Skaar EP,
590 and Crowe JE (2019). Human mAbs to Staphylococcus aureus IsdA Provide Protection Through Both
591 Heme-Blocking and Fc-Mediated Mechanisms. *J Infect Dis* 219(8)**,** 1264-1273. doi:
592 10.1093/infdis/jiy635.
593 Berends ET, Horswill AR, Haste NM, Monestier M, Nizet V, and von Kockritz-Blickwede M (2010). Nuclease
594 expression by Staphylococcus aureus facilitates escape from neutrophil extracellular traps. *J Innate*
595 *Immun* 2(6)**,** 576-586. doi: 10.1159/000319909.
596 Bravo-Santano N, Stolting H, Cooper F, Bileckaja N, Majstorovic A, Ihle N, Mateos LM, Calle Y, Behrends V, and
597 Letek M (2019). Host-directed kinase inhibitors act as novel therapies against intracellular
598 Staphylococcus aureus. *Sci Rep* 9(1)**,** 4876. doi: 10.1038/s41598-019-41260-8.
599 Brinkmann V, Reichard U, Goosmann C, Fauler B, Uhlemann Y, Weiss DS, Weinrauch Y, and Zychlinsky A (2004).
600 Neutrophil extracellular traps kill bacteria. *Science* 303(5663)**,** 1532-1535. doi:
601 10.1126/science.1092385.
602 Bunsow D, Tantawy E, Ostermeier T, Bahre H, Garbe A, Larsen J, and Winstel V (2021). Methicillin-resistant
603 Staphylococcus pseudintermedius synthesizes deoxyadenosine to cause persistent infection.
604 *Virulence* 12(1)**,** 989-1002. doi: 10.1080/21505594.2021.1903691.
605 Chambers HF, and Deleo FR (2009). Waves of resistance: Staphylococcus aureus in the antibiotic era. *Nat Rev*
606 *Microbiol* 7(9)**,** 629-641. doi: 10.1038/nrmicro2200.
607 Chen BY, Salas JR, Trias AO, Perez Rodriguez A, Tsang JE, Guemes M, Le TM, Galic Z, Shepard HM, Steinman L,
608 Nathanson DA, Czernin J, Witte ON, Radu CG, Schultz KA, and Clark PM (2022a). Targeting
609 deoxycytidine kinase improves symptoms in mouse models of multiple sclerosis. *Immunology*. doi:
610 10.1111/imm.13569.
611 Chen X, Schneewind O, and Missiakas D (2022b). Engineered human antibodies for the opsonization and killing
612 of Staphylococcus aureus. *Proc Natl Acad Sci U S A* 119(4). doi: 10.1073/pnas.2114478119.
613 Cheng AG, DeDent AC, Schneewind O, and Missiakas D (2011). A play in four acts: Staphylococcus aureus
614 abscess formation. *Trends Microbiol* 19(5)**,** 225-232. doi: 10.1016/j.tim.2011.01.007.
615 Dai J, Lai L, Tang H, Wang W, Wang S, Lu C, Yao H, Fan H, and Wu Z (2018). Streptococcus suis synthesizes
616 deoxyadenosine and adenosine by 5'-nucleotidase to dampen host immune responses. *Virulence* 9(1)**,**
617 1509-1520. doi: 10.1080/21505594.2018.1520544.
618 de Vor L, van Dijk B, van Kessel K, Kavanaugh JS, de Haas C, Aerts PC, Viveen MC, Boel EC, Fluit AC, Kwiecinski
619 JM, Krijger GC, Ramakers RM, Beekman FJ, Dadachova E, Lam MG, Vogely HC, van der Wal BC, van
620 Strijp JA, Horswill AR, Weinans H, et al. (2022). Human monoclonal antibodies against Staphylococcus
621 aureus surface antigens recognize in vitro and in vivo biofilm. *Elife* 11. doi: 10.7554/eLife.67301.
622 Duthie ES, and Lorenz LL (1952). Staphylococcal coagulase; mode of action and antigenicity. *J Gen Microbiol*
623 6(1-2)**,** 95-107. doi: 10.1099/00221287-6-1-2-95.
624 Finlay BB, and McFadden G (2006). Anti-immunology: evasion of the host immune system by bacterial and
625 viral pathogens. *Cell* 124(4)**,** 767-782. doi: 10.1016/j.cell.2006.01.034.

626 Foster TJ (2005). Immune evasion by staphylococci. *Nat Rev Microbiol* 3(12), 948-958. doi:
627 10.1038/nrmicro1289.
628 Fridkin SK, Hageman JC, Morrison M, Sanza LT, Como-Sabetti K, Jernigan JA, Harriman K, Harrison LH, Lynfield
629 R, and Farley MM (2005). Methicillin-resistant *Staphylococcus aureus* disease in three communities.
630 *N. Engl. J. Med.* 352, 1436-1444.
631 GBD 2019 Antimicrobial Resistance Collaborators (2022a). Global burden of bacterial antimicrobial resistance
632 in 2019: a systematic analysis. *Lancet* 399(10325), 629-655. doi: 10.1016/S0140-6736(21)02724-0.
633 GBD 2019 Antimicrobial Resistance Collaborators (2022b). Global mortality associated with 33 bacterial
634 pathogens in 2019: a systematic analysis for the Global Burden of Disease Study 2019. *Lancet*
635 400(10369), 2221-2248. doi: 10.1016/S0140-6736(22)02185-7.
636 Gudas LJ, Ullman B, Cohen A, and Martin DW, Jr. (1978). Deoxyguanosine toxicity in a mouse T lymphoma:
637 relationship to purine nucleoside phosphorylase-associated immune dysfunction. *Cell* 14(3), 531-538.
638 doi: 10.1016/0092-8674(78)90239-8.
639 Hua L, Hilliard JJ, Shi Y, Tkaczyk C, Cheng LI, Yu X, Datta V, Ren S, Feng H, Zinsou R, Keller A, O'Day T, Du Q,
640 Cheng L, Damschroder M, Robbie G, Suzich J, Stover CK, and Sellman BR (2014). Assessment of an anti-
641 alpha-toxin monoclonal antibody for prevention and treatment of Staphylococcus aureus-induced
642 pneumonia. *Antimicrob Agents Chemother* 58(2), 1108-1117. doi: 10.1128/AAC.02190-13.
643 Jian Z, Zeng L, Xu T, Sun S, Yan S, Yang L, Huang Y, Jia J, and Dou T (2021). Antibiotic resistance genes in bacteria:
644 Occurrence, spread, and control. *J Basic Microbiol* 61(12), 1049-1070. doi: 10.1002/jobm.202100201.
645 Kaufmann SHE, Dorhoi A, Hotchkiss RS, and Bartenschlager R (2018). Host-directed therapies for bacterial and
646 viral infections. *Nat Rev Drug Discov* 17(1), 35-56. doi: 10.1038/nrd.2017.162.
647 Kim HK, Emolo C, DeDent AC, Falugi F, Missiakas DM, and Schneewind O (2012). Protein A-specific monoclonal
648 antibodies and prevention of Staphylococcus aureus disease in mice. *Infect Immun* 80(10), 3460-3470.
649 doi: 10.1128/IAI.00230-12.
650 Klevens RM, Edwards JR, Gaynes RP, and National Nosocomial Infections Surveillance S (2008). The impact of
651 antimicrobial-resistant, health care-associated infections on mortality in the United States. *Clin Infect*
652 *Dis* 47(7), 927-930. doi: 10.1086/591698.
653 Klevens RM, Morrison MA, Nadle J, Petit S, Gershman K, Ray S, Harrison LH, Lynfield R, Dumyati G, Townes JM,
654 Craig AS, Zell ER, Fosheim GE, McDougal LK, Carey RB, and Fridkin SK (2007). Invasive methicillin-
655 resistant *Staphylococcus aureus* infections in the United States. *JAMA* 298, 1763-1771.
656 Kuehnert MJ, Kruszon-Moran D, Hill HA, McQuillan G, McAllister SK, Fosheim G, McDougal LK, Chaitram J,
657 Jensen B, Fridkin SK, Killgore G, and Tenover FC (2006). Prevalence of *Staphylococcus aureus* nasal
658 colonization in the United States, 2001-2002. *J. Infect. Dis.* 193, 172-179.
659 Le TM, Poddar S, Capri JR, Abt ER, Kim W, Wei L, Uong NT, Cheng CM, Braas D, Nikanjam M, Rix P, Merkurjev
660 D, Zaretsky J, Kornblum HI, Ribas A, Herschman HR, Whitelegge J, Faull KF, Donahue TR, Czernin J, et
661 al. (2017). ATR inhibition facilitates targeting of leukemia dependence on convergent nucleotide
662 biosynthetic pathways. *Nat Commun* 8(1), 241. doi: 10.1038/s41467-017-00221-3.
663 Lee AS, de Lencastre H, Garau J, Kluytmans J, Malhotra-Kumar S, Peschel A, and Harbarth S (2018). Methicillin-
664 resistant Staphylococcus aureus. *Nat Rev Dis Primers* 4, 18033. doi: 10.1038/nrdp.2018.33.
665 Liu P, Pian Y, Li X, Liu R, Xie W, Zhang C, Zheng Y, Jiang Y, and Yuan Y (2014). Streptococcus suis adenosine
666 synthase functions as an effector in evasion of PMN-mediated innate immunit. *J Infect Dis* 210(1), 35-
667 45. doi: 10.1093/infdis/jiu050.
668 Lowy FD (1998). Staphylococcus aureus infections. *N Engl J Med* 339(8), 520-532. doi:
669 10.1056/NEJM199808203390806.
670 Ma F, Guo X, and Fan H (2017). Extracellular Nucleases of Streptococcus equi subsp. zooepidemicus Degrade
671 Neutrophil Extracellular Traps and Impair Macrophage Activity of the Host. *Appl Environ Microbiol*
672 83(2). doi: 10.1128/AEM.02468-16.
673 McKenna M (2013). Antibiotic resistance: the last resort. *Nature* 499(7459), 394-396. doi: 10.1038/499394a.

674 Meka VG, and Gold HS (2004). Antimicrobial resistance to linezolid. *Clin Infect Dis* 39(7), 1010-1015. doi:
675 10.1086/423841.
676 Nubel U (2016). Emergence and Spread of Antimicrobial Resistance: Recent Insights from Bacterial Population
677 Genomics. *Curr Top Microbiol Immunol* 398, 35-53. doi: 10.1007/82_2016_505.
678 Okumura CY, and Nizet V (2014). Subterfuge and sabotage: evasion of host innate defenses by invasive gram-
679 positive bacterial pathogens. *Annu Rev Microbiol* 68, 439-458. doi: 10.1146/annurev-micro-092412-
680 155711.
681 Pai M, Behr MA, Dowdy D, Dheda K, Divangahi M, Boehme CC, Ginsberg A, Swaminathan S, Spigelman M,
682 Getahun H, Menzies D, and Raviglione M (2016). Tuberculosis. *Nat Rev Dis Primers* 2, 16076. doi:
683 10.1038/nrdp.2016.76.
684 Poddar S, Capparelli EV, Rosser EW, Gipson RM, Wei L, Le T, Jung ME, Radu C, and Nikanjam M (2020).
685 Development and preclinical pharmacology of a novel dCK inhibitor, DI-87. *Biochem Pharmacol* 172,
686 113742. doi: 10.1016/j.bcp.2019.113742.
687 Ragle BE, and Bubeck Wardenburg J (2009). Anti-alpha-hemolysin monoclonal antibodies mediate protection
688 against Staphylococcus aureus pneumonia. *Infect Immun* 77(7), 2712-2718. doi: 10.1128/IAI.00115-
689 09.
690 Reichard P (1988). Interactions between deoxyribonucleotide and DNA synthesis. *Annu Rev Biochem* 57, 349-
691 374. doi: 10.1146/annurev.bi.57.070188.002025.
692 Spaan AN, Surewaard BG, Nijland R, and van Strijp JA (2013). Neutrophils versus Staphylococcus aureus: a
693 biological tug of war. *Annu Rev Microbiol* 67, 629-650. doi: 10.1146/annurev-micro-092412-155746.
694 Tantawy E, Schwermann N, Ostermeier T, Garbe A, Bahre H, Vital M, and Winstel V (2022). Staphylococcus
695 aureus Multiplexes Death-Effector Deoxyribonucleosides to Neutralize Phagocytes. *Front Immunol* 13,
696 847171. doi: 10.3389/fimmu.2022.847171.
697 Thammavongsa V, Kern JW, Missiakas DM, and Schneewind O (2009). Staphylococcus aureus synthesizes
698 adenosine to escape host immune responses. *J Exp Med* 206(11), 2417-2427. doi:
699 10.1084/jem.20090097.
700 Thammavongsa V, Kim HK, Missiakas D, and Schneewind O (2015). Staphylococcal manipulation of host
701 immune responses. *Nat Rev Microbiol* 13(9), 529-543. doi: 10.1038/nrmicro3521.
702 Thammavongsa V, Missiakas DM, and Schneewind O (2013). Staphylococcus aureus degrades neutrophil
703 extracellular traps to promote immune cell death. *Science* 342(6160), 863-866. doi:
704 10.1126/science.1242255.
705 Thomsen IP, Sapparapu G, James DBA, Cassat JE, Nagarsheth M, Kose N, Putnam N, Boguslawski KM, Jones LS,
706 Wood JB, Creech CB, Torres VJ, and Crowe JE, Jr. (2017). Monoclonal Antibodies Against the
707 Staphylococcus aureus Bicomponent Leukotoxin AB Isolated Following Invasive Human Infection
708 Reveal Diverse Binding and Modes of Action. *J Infect Dis* 215(7), 1124-1131. doi: 10.1093/infdis/jix071.
709 Tong SY, Davis JS, Eichenberger E, Holland TL, and Fowler VG, Jr. (2015). Staphylococcus aureus infections:
710 epidemiology, pathophysiology, clinical manifestations, and management. *Clin Microbiol Rev* 28(3),
711 603-661. doi: 10.1128/CMR.00134-14.
712 Torres A, Cilloniz C, Niederman MS, Menendez R, Chalmers JD, Wunderink RG, and van der Poll T (2021).
713 Pneumonia. *Nat Rev Dis Primers* 7(1), 25. doi: 10.1038/s41572-021-00259-0.
714 von Kockritz-Blickwede M, and Winstel V (2022). Molecular Prerequisites for Neutrophil Extracellular Trap
715 Formation and Evasion Mechanisms of Staphylococcus aureus. *Front Immunol* 13, 836278. doi:
716 10.3389/fimmu.2022.836278.
717 Wenzel RP (2007). Health care-associated infections: major issues in the early years of the 21st century. *Clin*
718 *Infect Dis* 45 Suppl 1, S85-88. doi: 10.1086/518136.
719 Winstel V, Missiakas D, and Schneewind O (2018). Staphylococcus aureus targets the purine salvage pathway
720 to kill phagocytes. *Proc Natl Acad Sci U S A* 115(26), 6846-6851. doi: 10.1073/pnas.1805622115.
721 Winstel V, Schneewind O, and Missiakas D (2019). Staphylococcus aureus Exploits the Host Apoptotic Pathway
722 To Persist during Infection. *mBio* 10(6), e02270-02219. doi: 10.1128/mBio.02270-19.

723 Yaw LK, Robinson JO, and Ho KM (2014). A comparison of long-term outcomes after meticillin-resistant and
724 meticillin-sensitive Staphylococcus aureus bacteraemia: an observational cohort study. *Lancet Infect*
725 *Dis* 14(10)**,** 967-975. doi: 10.1016/S1473-3099(14)70876-X.
726 Zheng L, Khemlani A, Lorenz N, Loh JM, Langley RJ, and Proft T (2015). Streptococcal 5'-Nucleotidase A (S5nA),
727 a Novel Streptococcus pyogenes Virulence Factor That Facilitates Immune Evasion. *J Biol Chem*
728 290(52)**,** 31126-31137. doi: 10.1074/jbc.M115.677443.

729
730
731
732
733
734
735
736
737
738
739
740
741
742
743
744
745
746
747
748
749
750

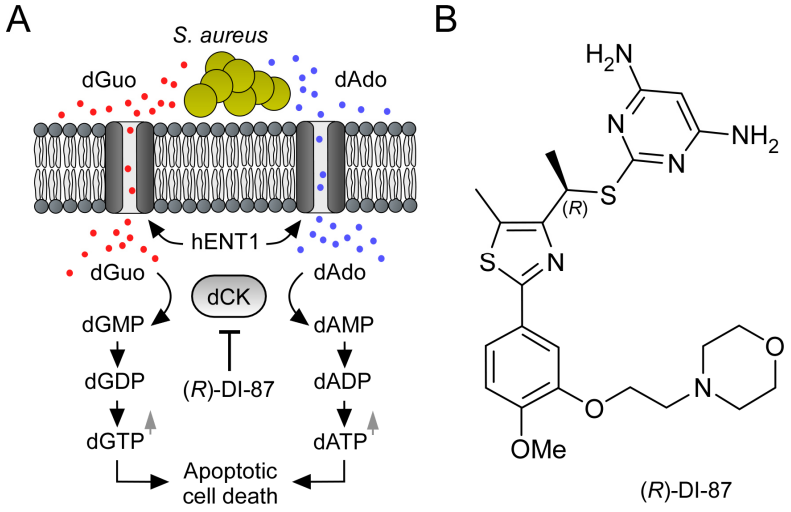

Figure 1. Mode of action of the dCK-specific inhibitor (*R*)-DI-87. (A) Scheme illustrating the mode of action of the dCK-specific inhibitor (*R*)-DI-87. *S. aureus*-derived dAdo and dGuo are pumped into phagocytes via human equilibrative transporter 1 (hENT1). Deoxycytidine kinase (dCK) converts dAdo and dGuo into appropriate deoxyribonucleoside monophosphates thereby triggering an accumulation of apoptosis-stimulating deoxyribonucleoside di- and triphosphates. (*R*)-DI-87 interferes with this pathway by inhibiting dCK, thus preventing host cell death. **(B)** Structure of (*R*)-DI-87.

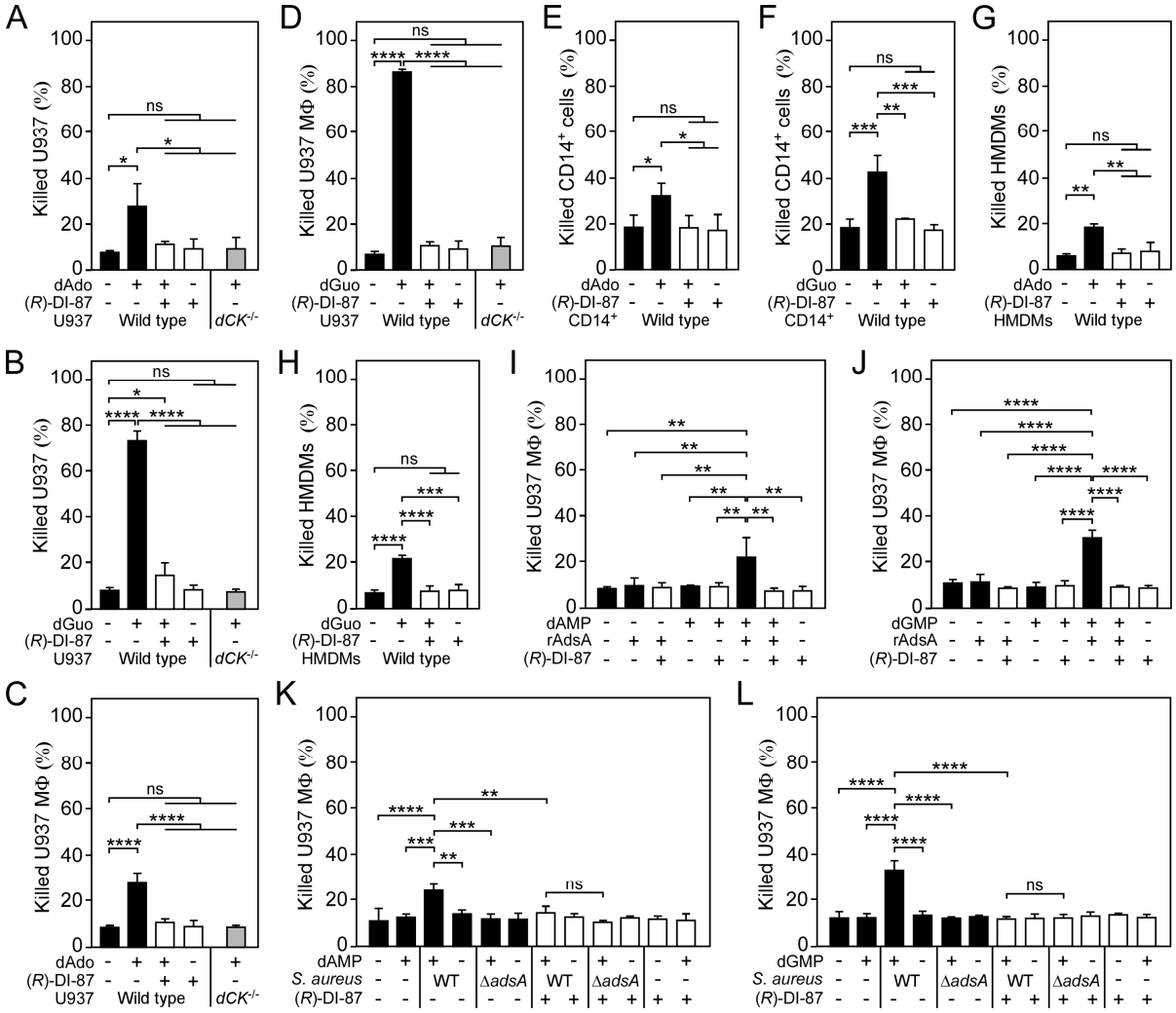

Figure 2. (*R*)-DI-87 protects phagocytes from death-effector deoxyribonucleoside-mediated cytotoxicity. (A-D) Survival rates of human U937 monocyte-like cells (U937) (A, B) or U937-derived macrophages (U937 MΦ) (C, D) exposed to dAdo or dGuo in the presence (+) or absence (-) of 1 µM (*R*)-DI-87. Cells were also exposed to the inhibitor or vehicle only. U937 *dCK*$^{-/-}$ were included as a control. **(E-H)** Survival rates of human CD14^{+} monocytes (E, F) or human monocyte-derived macrophages (HMDMs) (G, H) exposed to dAdo or dGuo in the presence (+) or absence (-) of 1 µM (*R*)-DI-87. Cells were also exposed to the inhibitor or vehicle only. **(I-J)** Survival rates of U937 MΦ exposed to rAdsA-derived dAdo (I) or dGuo (J). rAdsA was incubated with dAMP or dGMP and reaction products containing dAdo or dGuo were used to treat phagocytes in the presence (+) or absence (-) of 1 µM (*R*)-DI-87. Controls lacked rAdsA or deoxyribonucleoside monophosphates, or included reaction buffer only as indicated with + and − symbols. **(K, L)** Survival of vehicle- (-) or (*R*)-DI-87-exposed (+) U937 MΦ after treatment with culture medium (RPMI) that had been conditioned by incubation with either wild-type *S. aureus* Newman (WT) or its *adsA* mutant (Δ*adsA*) in the presence or absence of dAMP (K) or dGMP (L) as indicated with + and – symbols. Controls are indicated. 100 µM (A-B; E-F) or 200 µM (C-D; G-H) of dAdo or dGuo were used to treat the cells. Cell survival rates were analyzed 48 h (A-J) or 24 h (K, L) post-treatment. Data are the mean (± standard deviation [SD]) values from at least three independent determinations. Primary cell experiments include at least three independent donors. Statistically significant differences were analyzed by two-way (A-D) or one-way (E-L) analysis of variance (ANOVA) followed by Tukey's multiple-comparison test; ns, not significant ($P \geq 0.05$); *, $P < 0.05$; **, $P < 0.01$; ***, $P < 0.001$; ****, $P < 0.0001$.

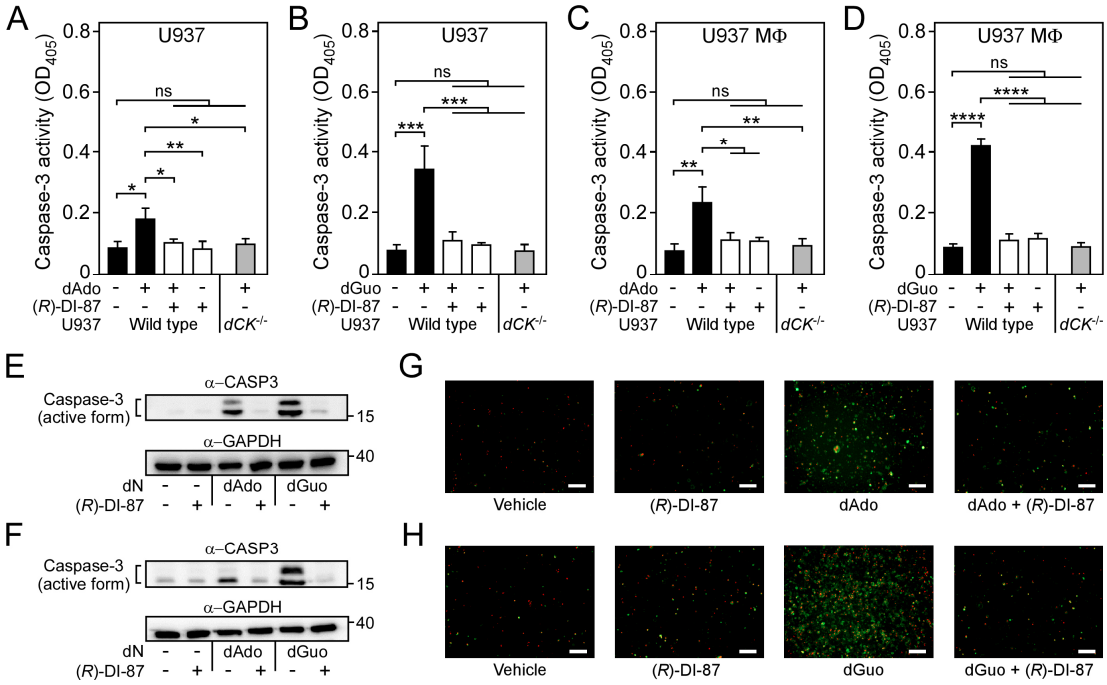

Figure 3. Selective inhibition of dCK prevents death-effector deoxyribonucleoside-mediated induction of immune cell apoptosis. (A-D) Analysis of caspase-3 activity in human U937 monocyte-like cells (U937) (A, B) or U937-derived macrophages (U937 MΦ) (C, D) exposed to dAdo or dGuo in the presence (+) or absence (-) of 1 µM (*R*)-DI-87. Cells were also exposed to the inhibitor or vehicle only. U937 *dCK*$^{-/-}$ were included as a control. Caspase-3 activity was analyzed using a colorimetric assay. **(E-F)** Immunoblotting of lysates obtained from U937 (E) or U937 MΦ (F) exposed to dAdo or dGuo in the presence (+) or absence (-) of 1 µM (*R*)-DI-87. Controls are indicated (+/– symbols). A specific antibody was used that can also detect the cleaved (active) form of caspase-3 (α-CASP3). GAPDH was used as a loading control (α-GAPDH). Numbers to the right of blots indicate the migration of molecular weight markers in kilodaltons. **(G-H)** Analysis of (*R*)-DI-87-dependent prevention of host cell apoptosis via immunofluorescence microscopy. U937 MΦ were exposed to dAdo (G) or dGuo (H) in the presence or absence of 1 µM (*R*)-DI-87 and stained using FITC-annexin-V/PI. Controls are indicated. White bars depict a length of 100 µm. Representative blots and images are shown. 100 µM (A-B; E) or 200 µM (C-D; F-H) of dAdo or dGuo were used to treat the cells. Apoptosis rates were analyzed 24 h post-treatment. Data are the mean (± standard deviation [SD]) values from three independent determinations. Statistically significant differences were analyzed by two-way analysis of variance (ANOVA) followed by Tukey's multiple-comparison test; ns, not significant ($P \geq 0.05$); *, $P < 0.05$; **, $P < 0.01$; ***, $P < 0.001$; ****, $P < 0.0001$.

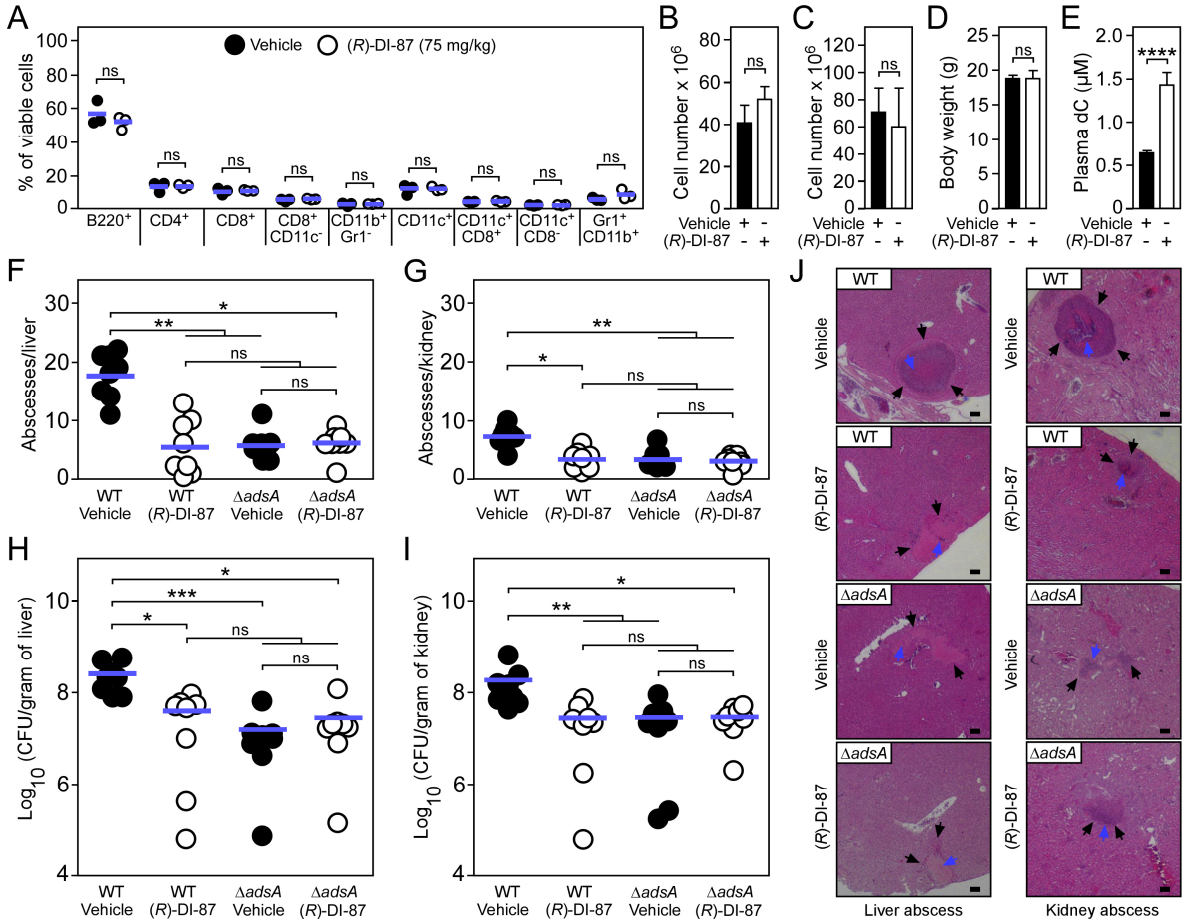

Figure 4. (*R*)-DI-87 protects against *S. aureus* invasive disease. (A-D) Safety assessment of (*R*)-DI-87 in mice. Cohorts of female C57BL/6 mice were treated with (*R*)-DI-87 (75 mg/kg) or vehicle (40% Captisol) via oral gavage in 12-hour intervals for 23 days. On day 16, peripheral blood was collected and subjected to a FACS-based immuno-phenotyping approach (A). Subsequent panels indicate the cellularity of spleen (B) and thymus (C) tissues along with the body weight of mice (D) on day 23. **(E)** Analysis of deoxycytidine (dC) content in mouse plasma following continuous dCK inhibitor treatment on day 23. **(F-I)** Enumeration of visible surface abscesses and staphylococcal loads in organs of *S. aureus*-challenged C57BL/6 mice treated with (*R*)-DI-87 (75 mg/kg) or vehicle (40% Captisol). Mice received (*R*)-DI-87 (75 mg/kg) or vehicle (40% Captisol) via oral gavage every 12 hours and were challenged with 10^7 CFU of wild-type *S. aureus* Newman (WT) or its *adsA* mutant (Δ*adsA*). Data for female C57BL/6 mice are displayed ($n = 8$). Bacterial burden was enumerated as $\log_{10}$ CFU per gram of tissue at 5 days post-infection. Horizontal blue bars represent the mean values of visible abscesses per organ (F-G) or indicate the mean CFU count in each cohort (H-I). **(J)** Microscopic images of H&E–stained liver or renal tissues obtained after necropsy of *S. aureus*-challenged C57BL/6 mice treated with (*R*)-DI-87 (75 mg/kg) or vehicle (40% Captisol). Mice received (*R*)-DI-87 (75 mg/kg) or vehicle (40% Captisol) via oral gavage every 12 hours and were challenged with 10^7 CFU of wild-type *S. aureus* Newman (WT) or its *adsA* mutant (Δ*adsA*). Arrows point to immune cell infiltrates (black) or replicating staphylococci (blue). Black bars depict a length of 100 μm. Representative images are shown. Statistically significant differences were analyzed by a two-tailed Student's t-test (A-E) or with the Kruskal–Wallis test corrected with Dunn's multiple comparison (F-I). ns, not significant ($P \geq 0.05$); *, $P < 0.05$; **, $P < 0.01$; ***, $P < 0.001$; ****, $P < 0.0001$.

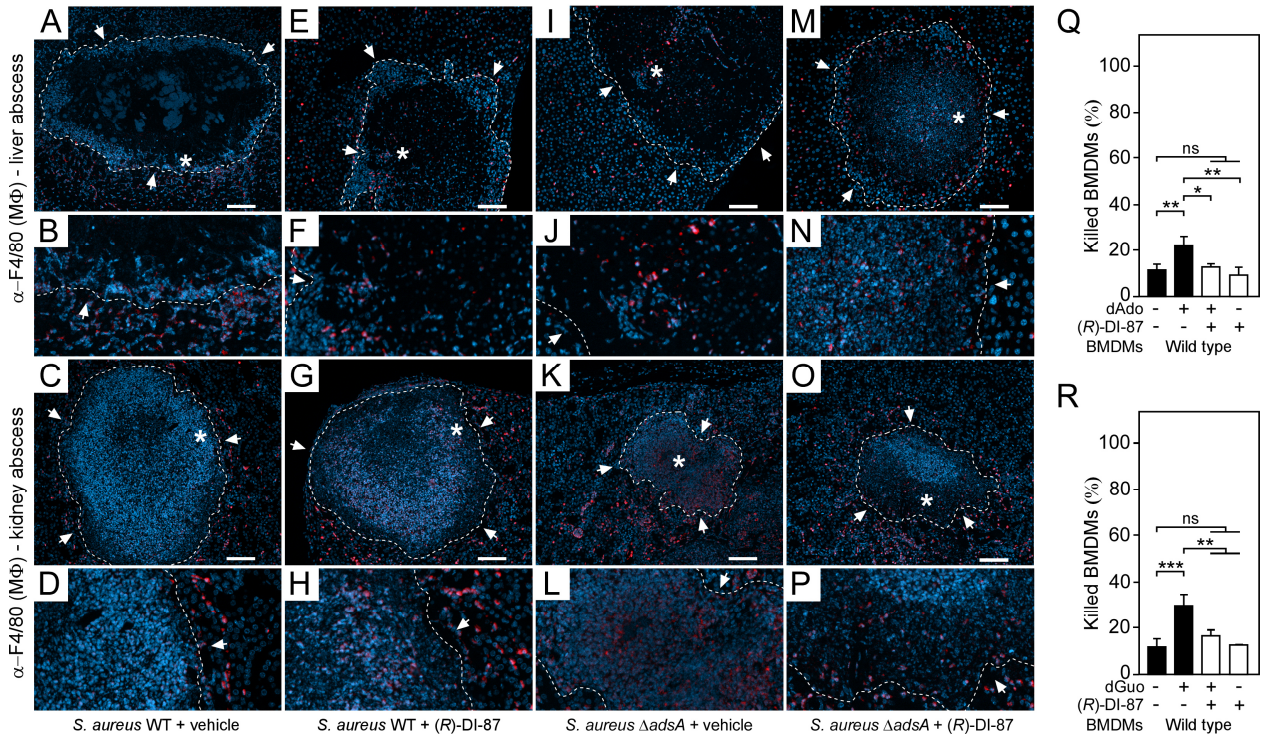

Figure 5. (*R*)-DI-87-mediated inhibition of dCK enhances macrophage infiltration into staphylococcal abscesses. (A-P) Immunofluorescence microscopy-based detection of macrophages in liver or renal tissues isolated 5 days after intravenous injection of 10^7 CFU of wild-type *S. aureus* Newman (WT) (A-H) or its *adsA* mutant (Δ*adsA*) (I-P) into female C57BL/6 mice treated with (*R*)-DI-87 (75 mg/kg) or vehicle (40% Captisol). Mice received (*R*)-DI-87 (75 mg/kg) or vehicle (40% Captisol) via oral gavage every 12 hours. White arrows point at the periphery of infectious foci (dashed lines). Magnifications of lesions from upper panels are indicated. Asterisk symbols define the region enlarged in the magnification counterpart images. Thin sections were stained with α-F4/80 antibodies (macrophages; red). Nuclei were labeled with DAPI (blue). White bars shown in the upper panels depict 100 µm length. Representative images are shown. **(Q, R)** Survival rates of female mice-derived bone marrow-derived macrophages (BMDMs) exposed to dAdo (Q) or dGuo (R) in the presence (+) or absence (-) of 1 µM (*R*)-DI-87. Cells were also exposed to the inhibitor or vehicle only. 200 µM of dAdo or dGuo were used to treat the cells. Cell survival rates were analyzed 48 h post-treatment. Data are the mean (± standard deviation [SD]) values from three independent determinations. Statistically significant differences were analyzed by one-way analysis of variance (ANOVA) followed by Tukey's multiple-comparison test; ns, not significant ($P \geq 0.05$); *, $P < 0.05$; **, $P < 0.01$; ***, $P < 0.001$.

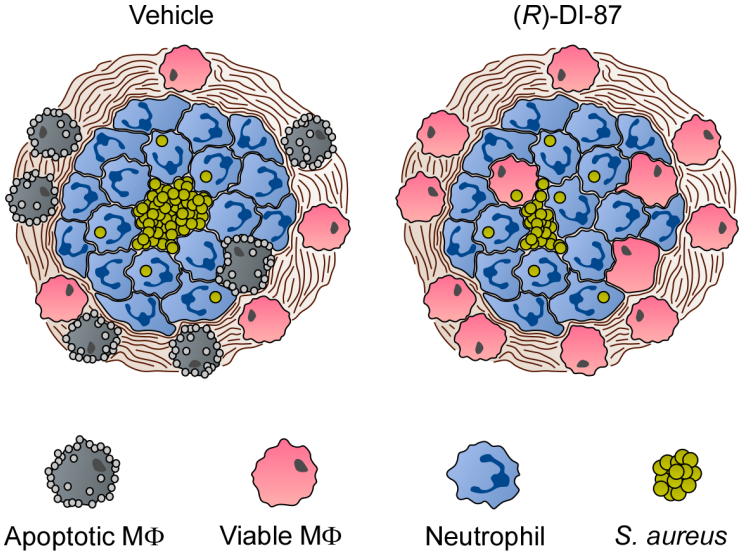

Figure 6. Proposed model of (*R*)-DI-87-mediated protection of phagocytes during *S. aureus* abscess formation. Diagram illustrating the (*R*)-DI-87-mediated protection of macrophages during the development of staphylococcal abscesses. While phagocytes get killed by *S. aureus*-derived death-effector deoxyribonucleosides in vehicle-treated animals, (*R*)-DI-87 protects macrophages and boosts their infiltration into the deeper cavity of infectious foci thereby enhancing eradication of staphylococci.